journal

J. Am. Ceram. Soc., 75 [12] 3305–14 (1992)

Consolidation Behavior of Flocculated Alumina Suspensions

Lennart Bergström,*,† Christopher H. Schilling,*,‡ and Ilhan A. Aksay*,§

Department of Materials Science and Engineering, University of Washington, Seattle, Washington 98195

Pacific Northwest Laboratory, Richland, Washington 99352

The consolidation behavior of flocculated alumina suspensions has been analyzed as a function of the interparticle energy. Consolidation was performed by a centrifugal force field or by gravity, and both the time-dependent and equilibrium density profiles were measured by a gamma-ray absorption technique. The interparticle energy at contact was controlled by adsorbing fatty acids of varying molecular weight at the alumina/decalin interface. We found that strongly attractive interactions result in a particle network which resists consolidation and shows compressible behavior over a large stress range. The most weakly flocculated suspension showed an essentially incompressible, homogeneous density profile after consolidation at different centrifugal speeds. We also found a significant variation in the maximum volume fraction, ϕ_m, obtained, with $\phi_m \approx 0.54$ for the most strongly flocculated suspension to $\phi_m \approx 0.63$ for the most weakly flocculated suspension. The compressive yield stresses show a behavior which can be fitted to a modified power law. In this paper, we discuss possible correlations between the fitting parameters and physical properties of the flocculated suspensions.

I. Introduction

INHOMOGENEITIES that originate in the particle-packing structures during shape forming of ceramic powders are important to control, since they can produce fracture origins in sintered materials or they can lead to shape distortion and cracking during drying, pyrolysis, and sintering. A better understanding of the evolution of the packing density during shape forming is needed to improve the reliability of the properties of sintered ceramics and also to advance new methods of processing complex shapes.

Several types of packing structure defects occur, depending on the shaping method used. For example, dry-pressing defects consist primarily of interagglomerate pores and packing density gradients that arise from die-wall friction and nonuniform stresses.[1,41] By comparison, shaping methods that involve the use of colloidal suspensions have a significant advantage in reducing inhomogeneities in particle packing, since the interparticle forces can be controlled by various means.[2] Regulating these forces can help to reduce inhomogeneities in the green microstructure by breaking up agglomerates, increasing the packing density uniformity, lowering the average pore size, and reducing the scale of mixing homogeneity.[3-5]

Measurements of the spatial variations of the packing density and mass segregation of both stable and flocculated suspensions have recently been reported. For example, electron microscopy studies by Chang *et al.*[32] showed that substantial mass segregation of a dispersed alumina–zirconia slurry took place during centrifugal consolidation. However, when a flocculated suspension was used instead, no mass segregation could be detected. Significant spatial variations in packing density were also detected by in situ radiography measurements during the pressure filtration of flocculated alumina, whereas, the use of the same, micrometer-sized alumina powder under dispersed conditions resulted in highly uniform packing.[6,36]

It is apparent that the degree to which density gradients are present in a given shaping process depends on two primary factors: (i) the compressive yield behavior of the particle network, which is controlled by the interparticle forces and the physical characteristics of the particles; and (ii) spatial variations of the stress on the particle network (the effective stress), that are inherent in the liquid removal process. For example, Buscall and White[12] and Auzerais *et al.*[13] have presented models for spatial variations of the effective stress in sediments. Tiller and co-workers have presented models for the slip casting[34] and the pressure filtration[35] process.

It is obvious that the state of the suspension (dispersed or flocculated) and the consolidation method employed have a significant influence on consolidation behavior. Generally, it is agreed in the ceramic engineering literature that dispersed slurries produce much higher average packing densities relative to strongly flocculated suspensions.[7,8] It has also been found that dispersed suspensions produce incompressible powder bodies, whereas flocculated suspensions produce a compressible powder body.[7,8] However, recent studies have shown that packing densities as high as those produced from stable suspensions can be attained by the use of certain additives, producing weakly flocculated suspensions. For example, Yin *et al.*[10] obtained high average packing densities by adding methacrylate polymers with different side groups to alumina in a nonpolar media. Similar effects were observed using polysiloxane additives in chloroform–alumina suspensions.[38] It has also been shown that although the addition of monovalent salt to an electrostatically stabilized alumina suspension flocculates the suspension, high average packing densities can be achieved.[10]

Although these earlier studies identify several chemistries which lead to high packing densities during consolidation, what is not particularly well understood are the effects of varying interparticle surface forces on macroscopic yielding in compression. It is believed that salt flocculation and the use of certain polymeric additives produce high packing densities because they provide short-range interparticle repulsion forces that screen the attractive van der Waals forces. Unfortunately, this hypothesis is difficult to verify because quantitative estimates of the interparticle forces cannot be obtained from the data reported in these studies.

The objective of this research is to systematically analyze the effect of varying the interparticle energy on the consolidation behavior of flocculated suspensions. In particular, two primary issues are addressed: (i) relating surface forces to density gradient evolution during centrifugal consolidation, and (ii) measuring fundamental relationships between surface forces and the

D. R. Clarke—contributing editor

Manuscript No. 195907. Received March 12, 1992; approved July 23, 1992.

Supported by the Foundation Blancheflor Boncampi-Ludovisi née Bildt and the Office of Basic Energy Sciences, U.S. Department of Energy, through a subcontract by Pacific Northwest Laboratory under Contract No. 063961-A-F1.

Pacific Northwest Laboratory is operated for the U.S. Department of Energy by Battelle Memorial Institute under Contract No. DE-AC06-76RLO1830.

*Member, American Ceramic Society.

†Permanent address where correspondence should be sent: Institute for Surface Chemistry, P.O. Box 5607, S-114 86, Stockholm, Sweden.

‡Pacific Northwest Laboratory.

§University of Washington.

macroscopic compressive yielding of flocculated particle networks. The interparticle energy at contact was controlled by adsorbing fatty acids of varying molecular weight at the alumina/solvent interface. By knowing the thickness of the steric barrier, the interparticle energy at contact can be estimated. Packing density gradients were determined by a gamma-ray absorption technique. This technique provides a method for analyzing the consolidation behavior that is relatively rapid, nondestructive, and requires a small number of samples to analyze yield behavior over a broad range of stresses and densities.

II. Theory of Centrifugal Consolidation

Models of batch settling under normal gravity for both stable and flocculated suspensions have been presented by several researchers.[11-14] We have modified these expressions by introducing centrifugal acceleration $\omega^2 z$, where ω is the angular velocity and z the distance from rotor center, in place of normal gravity acceleration g. The forces on a volume element of the suspension can be written as

$$-(U_s - U_l)/C(\phi) - \frac{\partial \sigma}{\partial z} + \Delta\rho\omega^2 z\phi = 0 \quad (1)$$

which is a modified Darcy equation. The first term in Eq. (1) represents the hydrodynamic resistance to consolidation caused by the upward flow of fluid. U_s is the local particle velocity and U_l is the local suspending fluid velocity. $C(\phi)$ is the hydraulic conductivity, which can be related to the permeability of the porous network. The second term is the stress-gradient of the network created by contact forces between the particles, where σ is the transmitted or effective stress. The third term is the net centrifugal force exerted on the suspended particles, where $\Delta\rho$ is the difference in mass density between the powder and the solvent and ϕ the volume fraction solids. The coordinate system is defined in Fig. 1. No wall stress was included in the model, as it was shown that the wall stress contribution could be ignored when containers of sufficiently large diameter were used.[15]

The conservation equation formulated by Kynch[16] gives

$$\frac{\partial \phi}{\partial t} + \frac{\partial [\phi U_s]}{\partial z} = 0 \quad (2)$$

If we assume that the stress transmitted between the particles is a unique function of the volume fraction of solids, ϕ, the spatial stress gradient can be expressed as

$$\frac{\partial \sigma}{\partial z} = \left(\frac{d\sigma}{d\phi}\right)\left(\frac{\partial \phi}{\partial z}\right) \quad (3)$$

Equations (1) through (3), together with no-flux conditions at the top and bottom of the centrifuge vessel and appropriately chosen boundary conditions, constitute a complete description of the centrifugal consolidation process.[14] In order to solve the resulting differential equation of the second order, we need to define the constitutive equations $C(\phi)$ and $\sigma(\phi)$. It is important to identify the qualitative difference between a colloidally stable suspension and a flocculated suspension. The stress σ transmitted between the particles in the colloidally stable case can be exchanged for the osmotic pressure π due to interparticle interactions. It was found, using results from molecular dynamic simulations for a hard-sphere suspension, that the osmotic pressure is negligible until random close packing is approached.[13] This is essentially the explanation for the incompressible nature of stable suspensions. However, if the particles are suspended in an aqueous solution at low ionic strength or if high molecular weight polymers are used to stabilize the system, a long-range "soft" repulsion would be introduced and, hence, the osmotic pressure could affect the consolidation behavior at much lower volume fractions.

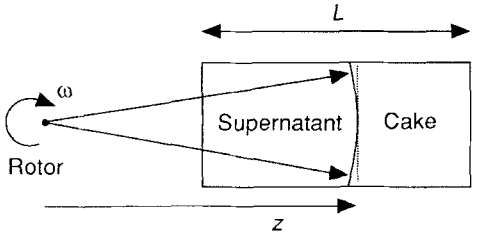

Fig. 1. Schematic illustration of the centrifuge experiments.

In a flocculated suspension, the aggregation process produces a volume-filling particle network at some critical volume fraction. This critical volume fraction may be as low as $\phi_g = 0.05$. Above ϕ_g, stress can be transmitted by particle–particle contacts throughout the network. It is commonly assumed that the particle network has a compressive yield stress which has to be exceeded in order for consolidation to occur.[13,14,37]

Hence, in Eq. (3), the transmitted stress σ is exchanged for the compressive yield stress σ_y for a flocculated suspension. Buscall *et al.*[33] investigated the compressive yield behavior of flocculated suspensions and found a power-law dependence of σ_y to ϕ. The functional form and the effect of the magnitude of the interparticle energy are, however, still unclear and will be addressed in this paper.

A second difference between a stable and a flocculated suspension is related to the functional form of the hydraulic conductivity $C(\phi)$. Because the hydraulic conductivity determines the kinetics of solid/liquid separation, a large number of empirical studies dealing with permeability as a function of volume fraction have been performed. However, it is still unclear how hydraulic conductivity (or permeability) varies with strength of flocculation and aggregate structure. Qualitatively, comparing two suspensions of the same volume fraction solids, it should be expected that the fractal nature of an aggregated particle network should lead to higher hydraulic conductivity, compared to the more homogeneous nature of a stable suspension. The fewer, larger pores between the flocs in the aggregated network constitute a smaller resistance to liquid flow, compared to the many, smaller pores between the single particles in a stable suspension.

III. Experimental

(1) Gamma-Ray Apparatus

A gamma-ray apparatus (Fig. 2) was used to nondestructively evaluate the suspension density as a function of elevation.[17,18] The apparatus directs a beam of gamma radiation from a Cs 137 isotope through a tube containing the suspension. The beam was collimated to 3.2 mm in diameter by passing it through bored holes in lead plates positioned in front of the isotope chamber and the germanium diode detector. Attenuation measurements were performed with a multichannel analyzer by integration of the energy as a function of intensity data at the photoelectric peak (662 keV).

At a given elevation, the average density within the irradiated portion of a sample can be calculated by using the Beer–Lambert law. Using this approach, it is necessary to determine the attenuation coefficients for the different phases. However, it was found that a simpler and more accurate approach is the use of a calibration curve.

Colloidally stable suspensions of alumina in decahydronaphthalene in the range 5 to 45 vol% solids were prepared by using the dispersant poly(12-hydroxy)stearic acid. Uniformity of the density of each sample was confirmed. Attenuation as a function of volume fraction was measured and resulted in a calibration curve

$$\phi_l = -0.5954 \ln (I/I_0) - 0.3279 \quad (4)$$

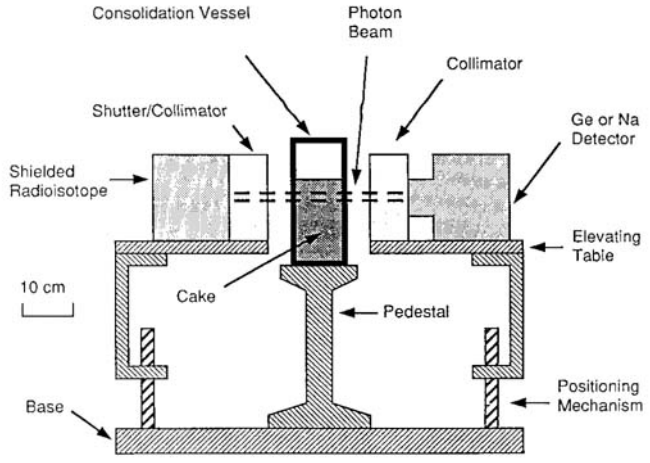

Fig. 2. Schematic drawing of the gamma-ray apparatus, from Ref. 17.

which was used in all the centrifugation experiments.

(2) *Experimental System*

In order to study the consolidation behavior quantitatively and to interpret the results regarding the effects of interparticle energies, a well-characterized powder system has to be used. A submicrometer alumina powder produced by spray pyrolysis of alkoxide droplets (AKP-30, Sumitomo Chemicals, Osaka, Japan) was chosen. The particle size distribution of a stable aqueous dispersion, measured by an X-ray absorption technique (Sedigraph 5000 E, Micromeritics, Norcross, GA) showed a mean particle diameter of 0.4 μm with 90% of the distribution within the size range 0.25 to 1.2 μm. Electron microscopy studies showed that the powder had an equiaxed morphology. The specific surface area measured by single-point BET with N_2 gas was 6.9 m^2/g. This value corresponds reasonably well with the calculated surface area of alumina spheres of radius 0.2 μm, indicating a nonporous powder. The density of the powder was 3.96 g/cm^3.

There are essentially two ways of controlling the magnitude of the total interparticle energy for flocculated systems. An attractive interaction induced by nonadsorbing polymer (depletion flocculation) can be used, where the molecular weight and the amount of polymer control the interaction energy. Another possibility is to provide some sort of screening of the ever-present van der Waals forces between the particles. This can be done, for example, by adsorbing surfactants, which have similar dielectric properties as the organic solvent, onto particles and provide thin steric barriers of varying thicknesses.[39] In this study, the latter method was used. Several studies have shown that fatty acids are strongly adsorbed onto alumina in organic media.[19–21] Because alumina particles are subject to relatively large van der Waals forces in most organic media, the interparticle energy at closest approach can be readily controlled by adsorbing fatty acids of varying molecular weights.

Decahydronaphthalene (decalin) was chosen as the solvent because of its low vapor pressure at room temperature (~1 mbar, $\sim 10^2$ Pa), limiting evaporation loss. The cyclic nature of the decalin molecule diminishes the risk of gelation due to induced attractive forces between the surfactant-coated particles and the solvent. Previous studies on silica dispersions stabilized by a grafted octadecyl layer showed that gelation could be induced by lowering the temperature to room temperature if the solvent was a long-chain alkane such as dodecane.[22] However, if the solvent was a cyclic alkane such as decalin, gelation was not induced until the temperature was lowered to nearly 0°C. Thus, as all the experiments were performed at room temperature (21° + 2°C), we assume that no additional attractive forces were induced. The density of the decalin used (anhydrous mixture of cis- and trans-decalin, 99+% from Aldrich Chemical Co., Milwaukee, WI) was 0.877 g/cm^3 measured by pychnometry. The refractive index was 1.475 and the static dielectric constant equaled 2.1.[23] The composition of the mixture of cis- and trans-isomers was estimated to 50/50, using a linear relationship between the composition and refractive index.[42]

(3) *Experimental Procedure*

Centrifugal experiments were carried out in polyacrylate tubes with an inner diameter of 7.62 cm. Each tube was fitted with an acrylic bottom plate sealed by a rubber O-ring. Because the floc structure and therefore the consolidation behavior is dependent on the initial shear history,[11,40] all suspensions were prepared following the same procedure. Also, the ingoing components, powder, fatty acids and solvent, were carefully pretreated or selected to keep the water content at a minimum. The powder was weighed into 400-mL glass beakers and vacuum dried overnight at 120°C. Anhydrous decalin was used as received, but the short fatty acids (propionic, pentanoic, and heptanoic acid) in liquid form were dried over 4-Å molecular sieves. Oleic acid was used as received. The dried powder was allowed to cool, mixed with the fatty acid and solvent, covered with aluminum foil, and mixed using a magnetic stirrer for 30 min. The amount of fatty acid added was estimated from the plateau value of the adsorption isotherms.[15] Measurements of the supernatants by acid–base titration after centrifugation showed remaining concentrations of fatty acids ranging from 1 to 5 m*M*. This shows that more than 90% of the added fatty acid was adsorbed at the alumina/decalin interface. Hence, centrifugation does not seem to influence the amount of fatty acid adsorbed.

The mixing was followed by ultrasonication for 10 min using a Sonic Materials Vibracell 600-W unit (Danbury, CT) and a 2.54-cm diameter high-gain ultrasonic horn. Each sample was cooled during ultrasonication by immersion in an ice bath. The ultrasonic treatment is believed to be sufficient to disrupt the initial powder aggregates and make it possible for the fatty acids to adsorb onto the surface of each primary particle. We checked this by following the above-described procedure, but, instead of adding a fatty acid, we used a steric stabilizer, poly(12-hydroxy)stearic acid, which has a carboxylic acid head group and a long hydrocarbon chain as a stabilizing tail. We found that the particle size distribution after ultrasonication was identical to the primary particle size distribution, showing that all agglomerates had been broken.

The suspension was left unstirred for approximately 15 min after ultrasonication and then poured into centrifuge tubes to an initial height of approximately 8.9 cm. The solids concentration was 20 vol% in all the centrifuge experiments. The tubes were centrifuged (International Centrifuge, size 2, International Equipment Company, Boston, MA) at centrifugal speeds between 550 and 2500 rpm. The distance from the rotor center to the bottom of the tube was 20.4 cm. The centrifugal speed was measured using an optical tachometer with high accuracy. After centrifugation, the cylindrical tube was removed from the centrifuge, put in the gamma-ray apparatus, and vertically aligned and centered before the volume fraction profile was measured. The centrifuge tube was then scanned in 2.5-mm steps, starting at the bottom. Any sort of drift or change during a measurement was checked by a final measurement of the attentuation of the pure solvent and by calculating the volume fraction solids. Values lower than ±0.5 vol% were accepted as random variation. The relative error was estimated to be 2%. Comparison of the calculations of the total volume fraction of powder deduced from the initial volume fraction and the initial suspension height and the measured total volume fraction confirmed the error estimate. The spatial resolution was estimated to be of the order of the diameter of the beam, hence about 3 to 4 mm.

(4) *Interaction Energies*

The theoretical interaction energies of two particles were calculated with the following expression:

$$V(D) = V_A(D) + V_S(D) \quad (5)$$

where $V_A(D)$ is the attractive van der Waals energy and $V_S(D)$ the repulsive steric energy. It was assumed that no additional interactions of electrostatic or structural origin were present. Although it has been reported that electrostatic effects can be induced in nonpolar solvents by addition of water,[43,44] the drying of powder, fatty acids, and solvent is expected to minimize these effects. The water absorption, which probably takes place during the preparation and centrifugation of the suspensions, is not sufficient to cause any charge buildup at the solid/liquid interface.

The van der Waals energy between two spheres of the same size is given by[24]

$$V_A(D) = -\frac{A_{eff}(D)}{6}\left[\frac{2a^2}{D^2 - 4a^2} + \frac{2a^2}{D^2} + \ln\left(\frac{D^2 - 4a^2}{D^2}\right)\right] \quad (6)$$

where D is the distance between the particle centers, a is the particle radius, and $A_{eff}(D)$ the effective Hamaker constant. An average particle radius of 0.2 μm was used in all calculations. The effective Hamaker constant was calculated using the simplified approach presented by Israelachvili,[25] and a nonretarded value of 4.9 kT (2.0×10^{-20} J) was obtained. Retardation effects were also included.[24]

$$A_{eff}(D) = \frac{3}{4}kT\left(\frac{\varepsilon(O)_1 - \varepsilon(O)_3}{\varepsilon(O)_1 + \varepsilon(O)_3}\right)^2 + \frac{3h\omega(n_1^2 - n_3^2)^2}{32\Pi\sqrt{2}(n_1^2 + n_3^2)^{1.5}}F(D) \quad (7)$$

$$F(D) = \left\{1 + \left[\frac{\pi n_3}{4\sqrt{2}}(n_1^2 + n_3^2)^{0.5}(D - 2a)\frac{\omega}{c}\right]^{1.5}\right\}^{-2/3} \quad (8)$$

$\varepsilon(O)_1$ and $\varepsilon(O)_3$ are the static dielectric constants for the particle and the media, respectively; n_1 and n_3 are the refractive index for the particles and media, respectively; and ω is the characteristic absorption frequency in the visible range. The following values were used: $\varepsilon(O)_1 = 11.6$, $n_1 = 1.752$ (Ref. 26), $\omega = 2.01 \times 10^{16}$ rad/s (Ref. 26), $\varepsilon(O)_3 = 2.15$, and $n_3 = 1.475$. We assumed that any van der Waals interaction between the adsorbed layers was negligible, as the dielectric properties are similar to the solvent properties. Hence, the attractive van der Waals interaction is occurring only between the alumina particle cores.

The steric interaction energy was calculated by[27,28]

$$V_S(D) = \frac{\pi a\, kT}{\bar{V}_3}\bar{\phi}_2^2\left(\frac{1}{2} - \chi\right)(2\delta + 2a - D)^2 \quad (9)$$

valid in the interpenetrational domain

$$\delta < (D - 2a) < 2\delta \quad (10)$$

This model assumes a constant density radially, of the adsorbed fatty acid layer, which is a reasonable approximation for thin dense layers. The precise choice of the values for the volume fraction of chains in the adsorbed layer $\bar{\phi}_2$, the partial molecular volume of decalin $\bar{V}_3$, and for the adsorbent–solvent interaction parameter χ is not so important, since the steric repulsive interaction increases rapidly when the distance of closest approach is below 2δ. Actually, the repulsive interaction could have been approximated to a hard-wall interaction, with a range δ from the particle surface, without changing the results to any significant extent. However, the following values were used: $\bar{\phi}_2 = 0.7$, $\bar{V}_3 = 2.6 \times 10^{-28}$ m^3, and $\chi = 0.35$. It could be argued that the volume fraction of the polymer in the adsorbed layer should decrease with increasing molecular weight because of the increase in area per molecule (Table I). However, as small variations in $\bar{\phi}_2$ did not cause any significant variation in the total interparticle energy curve, only one value was used.

The values of δ, the adsorbed layer thickness, were derived by equating the thickness with the fully extended chain length of the fatty acid. The chain lengths were estimated by building atomic models (CPK). The area per molecule (Table I) calculated from the plateau value of the adsorption isotherms[15] corresponds to the values of 20 to 25 Å^2 observed for densely packed fatty acids at the air/water interface.[29] Hence, the fatty acids form a densely packed layer at the alumina/decalin interface, with the carboxylic group attached to the alumina surface and the hydrocarbon tail extending into the solvent. The orientation of the fatty acids is assumed to be perpendicular to the surface. Since all the fatty acids used are in the liquid state at room temperature, there is probably a random fluctuation of the orientation. However, smaller changes in the orientation of the molecules and, hence, in the adsorbed layer thickness, result in insignificant changes in the calculated interaction energies.

The calculated total interaction energies for two alumina particles with different fatty acids adsorbed at the surface are shown in Fig. 3. The interaction energies for the different systems coincide at larger separation distances and become strongly repulsive at a distance determined by the thickness of the steric barrier. For each system, a maximum attractive energy ($-V_M$) can be defined, ranging from 54 kT for propionic acid to 11 kT for oleic acid. These values are summarized in Table I.

The calculations should be used only as an estimate of the interaction energies, since the powder used is polydisperse and not perfectly spherical and there are several inherent simplifications in the expressions for the attractive and repulsive interactions. However, we believe that, in spite of these shortcomings, the calculations in particular give a good estimate of the relative differences in interaction energy between the systems.

IV. Results and Discussion

(1) Transient Behavior

The effect of centrifugation time on the transient consolidation process was investigated by centrifuging a flocculated suspension at low speed (≈570 rpm). The suspension was first centrifuged for a prescribed time and then taken out from the centrifuge and the volume fraction profile was measured. This procedure was repeated until steady state was attained. The centrifuged cakes showed a curvature at the cake interface toward the pure solvent (Fig. 1). This is due mainly to the nonuniformity of the centrifugal forces across the centrifuge tube and may also be caused by wall effects. All the gamma-ray absorption measurements were performed in the direction of the "valley" created where the centrifugal forces are uniform across the tube. The centrifuge tube was carefully aligned in the same direction before each centrifuge run.

The results are summarized in Fig. 4 for a strongly flocculated suspension (pentanoic acid added, $V_M = -35$ kT). The suspensions showed an initial rapid consolidation, which continuously slowed. Steady state was not attained until ≥36 h centrifugation. After short centrifuge times (2 h), the suspension divided into three zones. A clear supernatant at the top was separated by a sharp interface from a constant density zone at approximately $\phi = 0.30$. At the bottom of the centrifuge tube there existed a consolidating zone with an increasing volume fraction towards the bottom. The volume fraction in the consolidating zone increased with time until steady state was reached after 36 h. At intermediate centrifuge times, the constant-density and the consolidating zones slowly merged until steady state was attained. At steady state, the volume fraction decreases towards the top of the cake due to the nonuniform stress field and the compressible nature of the particle network.

Some of these features can be explained qualitatively. The two forces resisting consolidation, as represented in Eq. (1), are

Table I. Estimated Thickness of the Steric Barrier, Area per Molecule Calculated from Adsorption Isotherms, and Calculated Interaction Energies[†]

Fatty acid	Thickness of steric barrier (nm)	Area per molecule (Å²)	Interaction energy (kT)
Propionic	0.7	19	−54
Pentanoic	1.0	22	−35
Heptanoic	1.2	23	−29
Oleic	2.5	31	−11

[†]Calculated at the distance of closest approach for two alumina spheres (a = 0.2 μm) with the different fatty acids acting as steric barriers at the alumina–decalin interface.

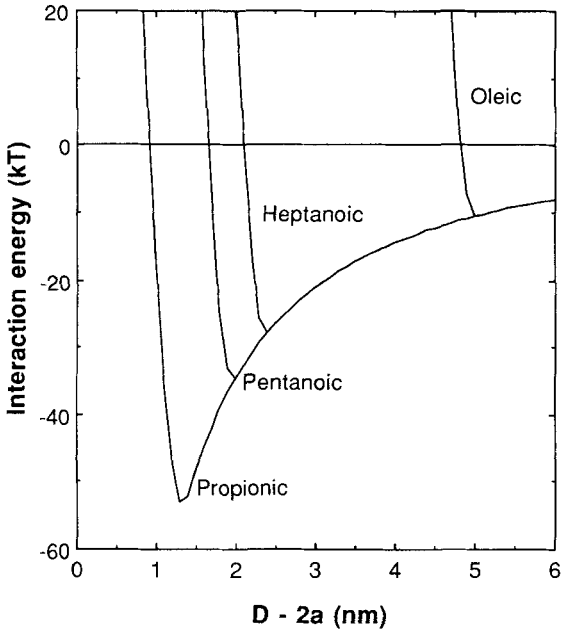

Fig. 3. Calculated interaction energies versus distance (D–$2a$) between alumina particles of radius a = 0.2 μm, immersed in decahydronaphthalene with different fatty acids providing a short-range steric repulsion.

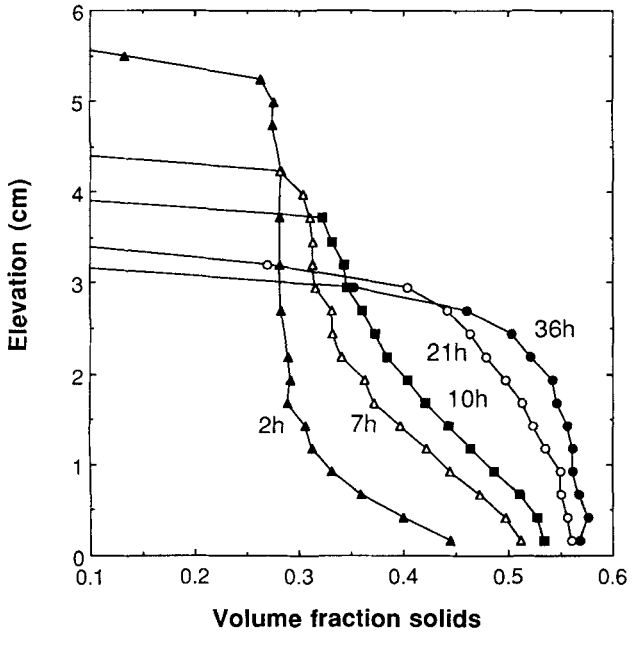

Fig. 4. Volume fraction profiles for a flocculated alumina suspension with pentanoic acid added (V_M = −35 kT) centrifuged at 570 ± 30 rpm at various times. ϕ_0 = 0.20 and the initial suspension height H_0 = 8.9 cm.

the hydrodynamic resistance, $(U_s - U_l)/C(\phi)$, and the particle network stress gradient, $d\sigma/dz$. When the consolidation rate decreases, the hydrodynamic resistance also decreases, which increases the stress on the particle network and, hence, leads to further consolidation. The consolidation rate decreases continuously until steady state is attained when the centrifugal force and the particle network stress gradient equal each other in every volume element.

In ceramic powder processing, high average green density and minimal density gradients are the desired goal. Hence, it is of paramount importance to reach steady state in centrifugal casting of flocculated suspensions in order to maximize the density and homogeneity of the cast green body. Although the total suspension height decreased marginally during the final stage of centrifugal consolidation, (i.e., between 21 and 36 h) it is evident from Fig. 4 that spatial variations of packing density were significantly reduced in this time period.

Auzerais *et al.*[13] have described a quantitative theory of the transient consolidation of stable and flocculated suspensions, which was briefly summarized in Section II. They showed that a diagram of dimensionless sediment height x^* versus dimensionless time t^* can be constructed for a system with defined particle interactions, initial volume fraction solids, and constitutive equations for permeability and particle network stress. In Fig. 5, such a plot is schematically shown. It can be seen that the system reaches equilibrium at a certain time, $t^* = t^*_{eq}$. The dimensionless settling time is defined as

$$t^* = \frac{tV_s}{L} \tag{11}$$

where L is the initial sediment height, t the absolute time, and V_s the Stokes expression for the sedimentation rate of an isolated sphere

$$V_s = \frac{2a^2\Delta\rho g}{9\eta} \tag{12}$$

where η is the viscosity of the medium. The dimensionless sediment height is defined as

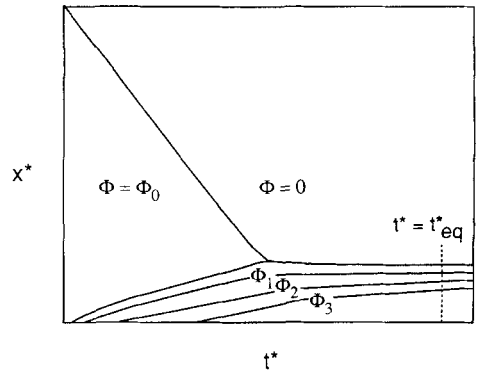

Fig. 5. Schematic settling behavior using the Auzerais *et al.* model,[13] showing lines of constant density for a flocculated suspension. Dimensionless sediment height x^* plotted against dimensionless time t^*. The sediment reaches steady state at $t^* = t^*_{eq}$.

$$X^* = X/L \tag{13}$$

where X is the absolute height.

If we assume that the model of Auzerais *et al.*[13] is also valid for centrifugal consolidation, it can be shown by using Eqs. (11) and (12) and using $g = \omega^2 R$ that the absolute time to reach steady-state t_{eq} should scale as

$$t_{eq} \sim \frac{L}{\omega^2 R} \tag{14}$$

for a defined system. Hence, a smaller initial suspension height or an increased centrifugal acceleration decreases the time to reach steady state.

However, the general validity of the model presented by Auzerais *et al.*[13] has not been established. Instead, recent experimental results on the transient settling in a gravitational field of flocculated suspensions of the same kind as used in this paper showed some deviation.[15]

What is unclear from the above analysis is how the specific parameters of the system such as particle interactions, suspension microstructure (porosity, permeability), particle size, and initial volume fraction also influence consolidation behavior. For example, the equilibration time should increase rapidly with a decrease in the particle size, due to decreased permeability.

Other studies on centrifugal casting of both dispersed and flocculated suspensions have been conducted recently.[30-32] Beylier *et al.*[30] studied time-dependent consolidation behavior by observing the position of the interface between the clear supernatant and the opaque dispersion for stable, submicrometer alumina suspensions. The use of this rather crude method showed that steady state was not attained until after several hours of centrifugation at 2500 g. Unfortunately, no information about the initial suspension height was given. In other studies on silicon nitride suspensions[31] and stable and salt-flocculated alumina and alumina/zirconia slurries,[32] it is not clear if steady state was achieved. With the initial suspension heights and centrifugal accelerations used in these latter experiments, there is a chance that steady state was not attained, due to the short centrifugation times.

Figures 6(A–D) show the steady-state volume fraction profiles at different centrifugal speeds. Repeated measurements showed that the results were reproducible. Each suspension was centrifuged for >38 h at approximately 600 rpm, and the volume fraction profile was measured. This procedure was then repeated by centrifuging the same suspension at 1000 rpm for 16 h and 2400 rpm for 3 h.

The most weakly flocculated suspension (oleic acid added, $V_M = -11$ kT) showed an essentially incompressible behavior with a constant volume fraction $\phi \approx 0.63$ at different centrifugal speeds (Fig. 6(D)). On the contrary, the most strongly flocculated suspension (propionic acid added, $V_M = -54$ kT) showed a highly compressible nature with an increasing volume fraction toward the bottom of the tube or with increasing centrifugal speed (Fig. 6(A)). The maximum volume fraction at the highest centrifugal speed, $\phi \approx 0.54$, was also lower. The other two suspensions with an intermediate degree of flocculation (Figs. 6(B) and (C)) showed a volume fraction gradient at low centrifugal speed but attained a constant volume fraction at the highest centrifugal speed.

Figure 7 shows the steady-state volume fraction profile of the different suspensions consolidated under normal gravity. The compressible nature of the particle network becomes obvious, as the applied stress is so much lower in this case.

(2) Compressive Yield Stresses

When steady state is attained, the hydrodynamic resistance represented by the first term in Eq. (1) vanishes. The particle network force and the centrifugal force field must then balance each other according to

$$\frac{\partial \sigma}{\partial z} = \Delta\rho\omega^2 z\phi \tag{15}$$

The stress in any volume element follows from integrating Eq. (15):

$$\sigma(z) = \Delta\rho\omega^2 \int_0^z x\phi(x)\,dx \tag{16}$$

Since we have measured the variation of volume fraction solids with elevation, a curve representing the compressive yield stress of the particle network versus volume fraction solids can be constructed.

Numerical integration of volume fraction profiles of the different suspensions spun at different speeds (Figs. 6(A–D)) were performed using Eq. (16). The volume fraction profiles of the sediments consolidated under normal gravity (Fig. 7) were also integrated using

$$\sigma(z) = \Delta\rho g \int_0^z \phi(x)\,dx \tag{17}$$

Figure 8 shows the calculated stress versus volume fraction solids for the four different systems. The curves have been plotted as volume fraction versus the logarithm of the compressive yield stress to allow direct comparison with similar curves obtained by dry pressing[1] or pressure filtration.[7] The low-stress end, up to ≈1 kPa, represents the consolidation under normal gravity. The high-stress end, from 50–70 kPa to ≈0.5 MPa, represents the steady-state behavior in a centrifugal force field. In every numerical integration, the stress values representing the top of the cake were removed, due to uncertain attenuation measurements.

A striking result from the comparisons of the plots is that all systems exhibit an asymptotic approach to a maximum volume fraction, ϕ_m, that is dependent on the interparticle energy. The maximum volume fraction decreases with an increase in the magnitude of the attractive interparticle energy and varies between $\phi_m = 0.63$ ($V_M = -11$ kT) and $\phi_m = 0.54$ ($V_A = -54$ kT) (Fig. 9). The most weakly flocculated suspension (oleic acid added, $V_M = -11$ kT) shows a maximum volume fraction close to random close packing of spheres ($\phi = 0.64$). However, it should be remembered that the measured volume fractions represent only the volume fraction of alumina. When packing particles, the volume of the adsorbed layer should also be included. If the adsorbed fatty acid layer is assumed incompressible, the maximum volume fraction of powder and oleic acid together is increased to $\phi_m \sim 0.65$. For the other systems with thinner adsorbed layers, this effect on the maximum volume fraction is less than 1 vol%.

Another factor that should be considered is the particle size. Buscall *et al.*[33] showed that the compressive yield stress increases rapidly with a decrease in particle size. Since the present study investigated only one type of powder, no particle size effects could be elucidated. It is also of interest to mention that the suspension with oleic acid added exhibits quite plastic shearing behavior, based on qualitative hand-molding tests. This directly contrasts with dispersed systems that are traditionally used to create high densities but usually exhibit a dilatant, brittle behavior.

From our experimental results, it is quite clear that global consolidation behavior cannot be described by a function of the form $\phi \sim \log \sigma$. This popular exponential relation can perhaps describe the consolidation behavior in a small stress range but fails when the stress range is expanded. In particular, a stress–volume fraction relation needs to account for the asymptotic approach to a maximum volume fraction.

We have used an empirical expression of the form

$$\sigma_y(\phi) = \frac{\sigma_0 \phi^n}{(\phi_m - \phi)} \tag{18}$$

where ϕ_m is the maximum volume fraction solids, σ_0 is a constant specific for the system, and n can vary between 2 and 5.[13]

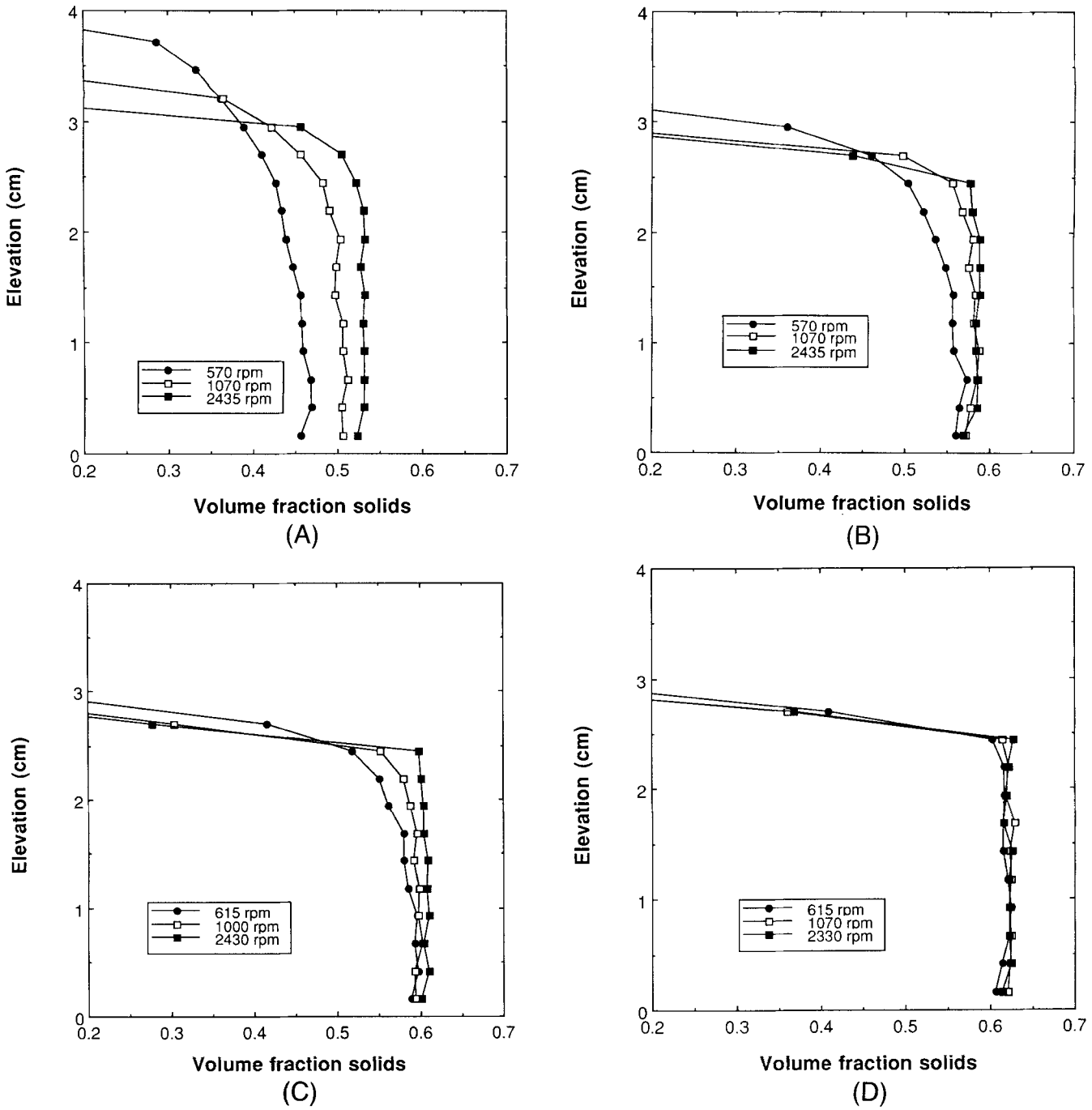

Fig. 6. Volume fraction profiles at steady state for flocculated alumina suspensions with different fatty acids added: (A) propionic acid added ($V_M = -54$ kT), (B) pentanoic acid added ($V_M = -35$ kT), (C) heptanoic acid added ($V_M = -29$ kT), (D) Oleic acid added ($V_M = -11$ kT). Each suspension was centrifuged at three rotational speeds at $\phi_0 = 0.20$.

The best fits for the different suspensions are shown in Fig. 8, with the fitting parameters tabulated in Table II.

If the low-stress end of the empirical fit is examined more closely, it can be found that the two most weakly flocculated suspensions (oleic and heptanoic acid added) show a good fit, whereas the two most strongly flocculated suspensions (propionic and pentanoic acid added) show some deviation. The settling measurements under normal gravity which represent this stress range were performed with an initial volume fraction of $\phi_0 = 0.15$. As this initial volume fraction lies above the critical gel-forming concentration ($\phi_g \approx 0.10$), there exists a zone for the strongly flocculated suspensions where the compressive stress never will exceed the yield stress at the initial volume fraction. This may explain the flat, low-stress end of the experimental curve for the suspension with propionic acid added. No such unconsolidated region exists for the weakly flocculated suspensions (oleic and heptanoic acid added), and hence the fit to Eq. (18) is much better. A lower critical volume fraction can be introduced in an empirical relation, e.g., as

$$\sigma_y(\phi) = \frac{\sigma_0(\phi - \phi_g)^n}{(\phi_m - \phi)} \tag{19}$$

which probably should result in a better fit for the low-stress end. However, in the context of ceramic processing we are interested mainly in the compressive behavior at high-volume fractions, and thus no such attempt was made.

No theoretical model of $\sigma_y(\phi)$ exists at the moment; hence, the physical significance of n and σ_0 is unclear. However, we have attempted to compare the yield stress behavior to other related phenomena in order to draw some conclusions about the

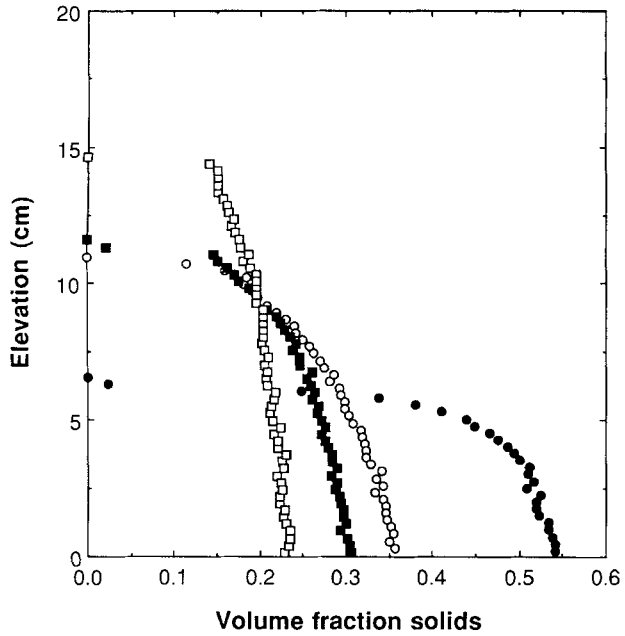

Fig. 7. Volume fraction profiles at steady state for alumina suspensions, with (□) propionic acid, (■) pentanoic acid, (○) heptanoic acid, and (●) oleic acid added. The suspensions were consolidated under normal gravity with $\phi_0 = 0.15$.

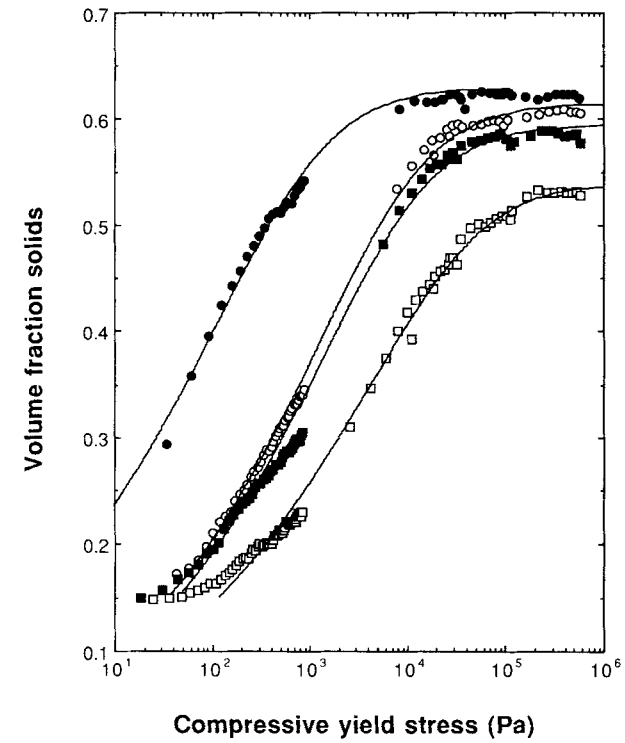

Fig. 8. Effect of the calculated compressive yield stress on the packing density of flocculated alumina suspensions with various interparticle energies (□, $V_M = -54$ kT; ■, $V_M = -35$ kT; ○, $V_M = -29$ kT; ●, $V_M = -11$ kT). The experimental points were fitted to a modified power law (see Table II).

relationship between the power-law exponent n, the preexponential factor σ_0, and the physical characteristics of the system. The power-law exponent n shows only a small variation, $n = 3.0$ to 3.4 between the different suspensions (Table II). This scaling can be compared to the results obtained by Buscall *et al.*,[33] where they derived compressive yield stresses of flocculated silica and polystyrene particle networks from curves of

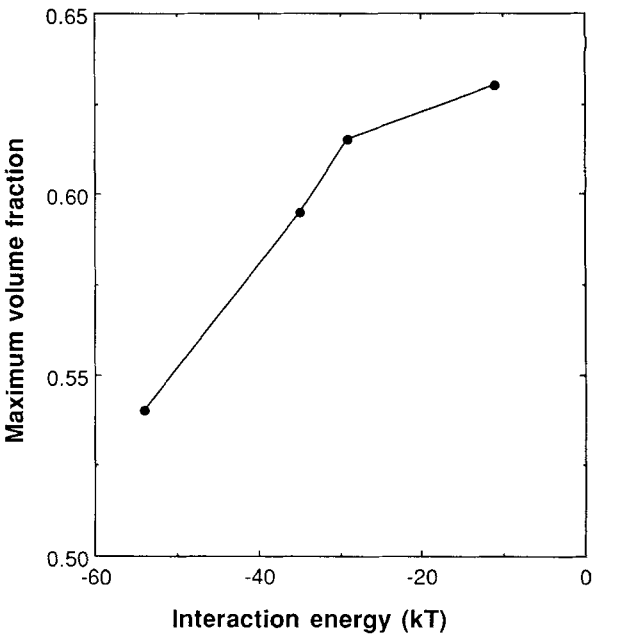

Fig. 9. The effect of the magnitude of the interparticle energy, V_M, on the maximum packing density of flocculated alumina suspensions.

equilibrium sediment height versus g-value. The data were fitted to a power law, $\sigma_y \sim \phi^n$, with $n = 4 \pm 0.5$. Observe that they studied only suspensions up to a concentration $\phi \sim 0.3$ and did not incorporate any modification for the asymptotic approach to a maximum volume fraction (see Eq. (18)). They compared their results with a model of the elasticity modulus, G, of a network of interconnected fractal clusters which predicted $G \sim \phi^\mu$, where the power-law exponent μ depends on the type of aggregation. If we assume that the compressive yield stress scales in direct proportion to the modulus, then $\mu = n$.

Hence, our results indicate the possibility of a fractal particle structure. Also, due to the small variation in n, it is possible that there are only small variations in the network microstructure between the different suspensions.

With the assumption of a similar microstructure between the different suspensions, it is tempting to relate σ_0 to the magnitude of the particle–particle energy ($-V_M$). A log–log plot (Fig. 10) gives a slope of 2.4, which indicates a scaling of the form

$$\sigma_0 \sim (-V_M)^{2.4} \tag{20}$$

Buscall *et al.*[28] related the Bingham yield stress, obtained by rheological measurements, to the magnitude of the attractive interaction energy for weakly flocculated suspensions and obtained a scaling with the exponent 1.9, similar to our results. However, it is important to emphasize again that until a theoretical model of $\sigma_y(\phi)$ exists, the relation of the fitting parameters to physical entities will remain unclear.

V. Summary and Conclusions

The centrifugal consolidation behavior of flocculated alumina suspensions is strongly affected by the degree of flocculation. Strongly attractive interactions result in a particle network which resists consolidation and shows a compressible behavior over a large stress range. We have measured the volume fraction profiles of four suspensions with different degrees of flocculation and found large spatial variations in packing density for the strongly flocculated suspension, whereas the most weakly flocculated suspension showed an essentially incompressible, homogeneous density profile. Smaller spatial variations in the packing density were obtained by increasing the centrifugal acceleration. However, the maximum volume

Table II. Parameters with the Best Fit to the Stress–Density Results Shown in Fig. 8 by Using an Empirical Expression of the Form $\sigma = (\sigma_0\phi^n)/(\phi_m - \phi)$

Fatty acid	ϕ_m	n	σ_0 (Pa)
Propionic	0.54	3.4 ± 0.2	2.8 ± 0.5 × 10^4
Pentanoic	0.595	3.0 ± 0.2	6.0 ± 1.4 × 10^3
Heptanoic	0.615	3.0 ± 0.2	5.2 ± 1.1 × 10^3
Oleic	0.63	3.4 ± 0.2	5.3 ± 1.1 × 10^2

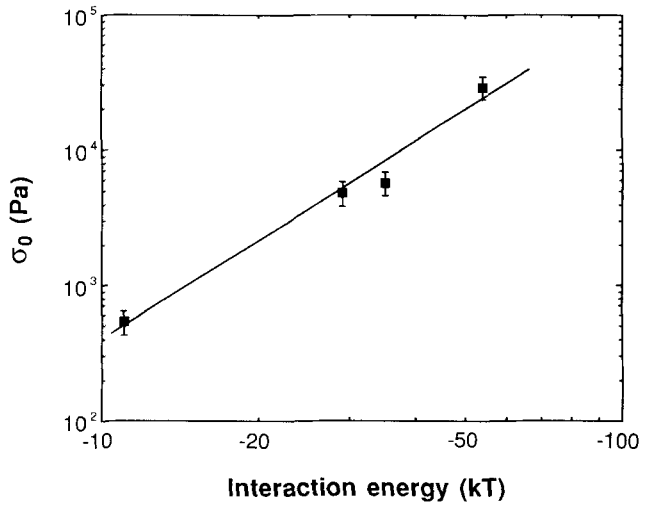

Fig. 10. Log–log plot of the preexponential factor σ_0 against the magnitude of the interparticle energy, V_M.

fraction solids obtained showed a strong dependence on the interaction energy. The maximum volume fraction varied from $\phi_m \approx 0.54$ for the most strongly flocculated suspension to $\phi_m \approx 0.63$ for the most weakly flocculated suspension.

Compressive yield stresses, calculated through numerical integration of the volume fraction profiles at steady state, show a behavior which can be fitted with a modified power law. The small variation of the power-law exponent indicates that there are insignificant differences in the network microstructure between the different suspensions. The preexponential factor could then be related to the magnitude of the interparticle energy, and a relation $\sigma_0 \sim (-V_M)^{2.4}$ was found. The widely used exponential expression $\phi \sim \log \sigma$, although valid over a narrow stress range, could not describe the global compressive yield behavior of these flocculated suspensions.

Acknowledgments: The authors wish to thank L. Thompson and H. L. Ker for technical assistance.

References

[1]N. G. Stanley-Wood, *Enlargement and Compaction of Particulate Solids*. Butterworths, London, U.K., 1983.

[2]R. G. Horn, "Surface Forces and Their Action in Ceramic Materials," *J. Am. Ceram. Soc.*, **73** [5] 1117–35 (1990).

[3]I. A. Aksay, "Microstructure Control through Colloidal Consolidation"; pp. 94–104 in Advances in Ceramics, Vol. 9, *Forming of Ceramics*. Edited by J. A. Mangels and G. L. Messing. American Ceramic Society, Westerville, OH, 1984.

[4]I. A. Aksay, "Principles of Ceramic Shape Forming with Powder Systems"; pp. 663–74 in Ceramic Transactions, Vol. 1, *Ceramic Powder Science II*. Edited by G. L. Messing, E. R. Fuller, Jr., and H. Hausner. American Ceramic Society, Westerville, OH, 1988.

[5]F. F. Lange, "Powder Processing Science and Technology for Increased Reliability," *J. Am. Ceram. Soc.*, **72,** 3–15 (1989).

[6]C. H. Schilling, W.-H. Shih, W. Y. Shih, and I. A. Aksay, "Advances in the Drained Shaping of Ceramics"; pp. 307–20 in Ceramic Transactions, Vol. 22, *Ceramic Powder Science IV*. Edited by S. Hirano, G. L. Messing, and H. Hausner. American Ceramic Society, Westerville, OH, 1991.

[7]F. F. Lange and K. T. Miller, "Pressure Filtration: Consolidation Kinetics and Mechanics," *Am. Ceram. Soc. Bull.*, **66,** 1498–504 (1987).

[8]J. F. A. K. Kotte, J. A. M. Denissen, and R. Metselaar, "Pressure Casting of Silicon Nitride," *J. Eur. Ceram. Soc.*, **7,** 307–14 (1991).

[9]B. V. Velamakanni, J. C. Chang, F. F. Lange, and D. S. Pearson, "New Method for Efficient Colloidal Particle Packing via Modulation of Repulsive Lubricating Hydration Forces," *Langmuir*, **6,** 1323–25 (1990).

[10]T. K. Yin, I. A. Aksay, and B. E. Eichinger, "Lubricating Polymers for Powder Compaction"; see Ref. 4, pp. 654–62.

[11]F. M. Tiller and Z. Khatib, "Theory of Sediment Volumes of Compressible, Particulate Structures," *J. Colloid Interface Sci.*, **100,** 55–67 (1984).

[12]R. Buscall and L. R. White, "The Consolidation of Concentrated Suspensions. 1. The Theory of Sedimentation," *J. Chem. Soc., Faraday Trans. 1*, **83,** 873–91 (1987).

[13]F. M. Auzerais, R. Jackson, and W. B. Russel, "The Resolution of Shocks and the Effects of Compressible Sediments in Transient Settling," *J. Fluid Mech.*, **195,** 437–62 (1988).

[14]R. Buscall, "The Sedimentation of Concentrated Colloidal Suspensions," *Colloids Surf.*, **43,** 33–53 (1990).

[15]L. Bergström, "Sedimentation of Flocculated Alumina Suspensions: Gamma-ray Measurements and Comparison to Model Predictions," *J. Chem. Soc., Faraday Trans.*, in press.

[16]G. J. Kynch, "A Theory of Sedimentation," *Trans. Faraday Soc.*, **48,** 166–76 (1952).

[17]C. H. Schilling, G. L. Graff, W. D. Samuels, and I. A. Aksay, "Gamma-ray Densitometry: Nondestructive Analysis of Density Evolution during Ceramic Powder Processing"; pp. 239–51 in *Atomic and Molecular Processing of Electronic and Ceramic Materials: Preparation, Characterization and Properties*, MRS Conference Proceedings. Edited by I. A. Aksay, G. L. McVay, T. G. Stoebe, and J. F. Wager. Materials Research Society, Pittsburgh, PA, 1988.

[18]C. H. Schilling and I. A. Aksay, "Gamma-ray Attenuation Analysis of Packing Structure Evolution during Powder Consolidation"; see Ref. 4, pp. 800–808.

[19]J. J. Kipling and E. H. M. Wright, "The Adsorption of Stearic Acid from Solution by Oxide Adsorbents," *J. Chem. Soc.*, 3535–3540 (1964).

[20]J. H. de Boer, G. M. M. Houben, B. C. Lippens, W. H. Meijs, and W. K. A. Walrave, "Study of the Nature of Surfaces with Polar Molecules. 1. Adsorption of Lauric Acid on Aluminum Oxides and Hydroxides," *J. Catal.*, **1,** 1–7 (1962).

[21]H. Hasegawa and M. J. D. Low, "Infrared Study of Adsorption in situ at the Liquid–Solid Interface. 3. Adsorption of Stearic Acid on Silica and on Alumina and of Decanoic Acid on Magnesia," *J. Colloid Interface Sci.*, **30,** 378–86 (1969).

[22]J. W. Jansen, G. G. de Kruif, and A. Vrij, "Attractions in Sterically Stabilized Silica Dispersions. 2. Experiments on Phase Separation Induced by Temperature Variations," *J. Colloid Interface Sci.*, **114,** 481–91 (1986).

[23]*Cis- and Trans-Decalin*, API Monograph Series, API Publication 706. American Petroleum Institute, Washington, DC, October, 1978.

[24]W. B. Russel, D. A. Saville and W. R. Schowalter, *Colloidal Dispersions*, Ch. 5. Cambridge Press, Cambridge, U.K., 1989.

[25]J. Israelachvili, *Intermolecular and Surface Forces*. Academic Press, London, U.K., 1985.

[26]D. B. Hough and L. R. White, "The Calculation of Hamaker Constants from Lifshitz Theory with Applications to Wetting Phenomena," *Adv. Colloid. Interface Sci.*, **14,** 3–41 (1980).

[27]D. H. Napper, *Polymeric Stabilization of Colloidal Dispersions*. Academic Press, London, U.K., 1983.

[28]R. Buscall, I. J. McGowan, and C. A. Mumme-Young, "Rheology of Weakly-Interacting Colloidal Particles at High Concentrations," *Faraday Discuss. Chem. Soc.*, **90,** 115–127 (1991).

[29]J. T. Davies and E. K. Rideal, *Interfacial Phenomena*. Academic Press, New York, 1963.

[30]E. Beylier, R. L. Pober, and M. J. Cima, "Centrifugal Casting of Ceramic Components"; pp. 529–36 in Ceramic Transactions, Vol. 12, *Ceramic Powder Science III*. Edited by G. L. Messing, S. Hirano, and H. Hausner. American Ceramic Society, Westerville, OH, 1990.

[31]O. Lyckfeldt, R. Pompe, and E. Lidén, "Non-aqueous, Centrifugal Casting of Silicon Nitride"; see Ref. 6, pp. 329–34.

[32]J. C. Chang, B. V. Velamakanni, F. F. Lange, and D. S. Pearson, "Centrifugal Consolidation of Al_2O_3 and Al_2O_3/ZrO_2 Composite Slurries vs Interparticle Potentials: Particle Packing and Mass Segregation," *J. Am. Ceram. Soc.*, **74,** 2201–204 (1991).

[33]R. Buscall, P. D. A. Mills, J. W. Goodwin, and D. W. Lawson, "Scaling Behavior of the Rheology of Aggregate Networks Formed from Colloidal Particles," *J. Chem. Soc., Faraday Trans. 1*, **84,** 4249–60 (1988).

[34]F. M. Tiller and C. D. Tsai, "Theory of Filtration of Ceramics: I. Slip Casting," *J. Am. Ceram. Soc.*, **69,** 882–87 (1986).

[35]F. M. Tiller and C. S. Yeh, "Relative Liquid Removal in Filtration and Expression," *Filtr. Sep.*, **27,** 129–35 (1990).

[36]W.-H. Shih, S. I. Kim, W. Y. Shih, C. H. Schilling, and I. A. Aksay, "Consolidation of Colloidal Suspensions"; pp. 167–77 in *Better Ceramics through*

Chemistry IV, MRS Symposium Proceedings, Vol. 180. Edited by B. J. J. Zelinski, C. J. Brinker, D. E. Clark, and D. R. Ulrich. Materials Research Society, Pittsburgh, PA, 1990.

[37]A. S. Michaels and J. C. Bolger, "Settling Rates and Sediment Volumes of Flocculated Kaolin Suspensions," *Ind. Eng. Chem. Fundam.*, **1,** 24–33 (1962).

[38]C. H. Schilling, W.-H. Shih, J. J. Lannutti, and I. A. Aksay, "Stress Density Variations in Alumina Sediments: Effects of Polymer Chemistry"; pp. 151–61 in *Mechanical Properties of Porous and Cellular Materials*, MRS Symposium Proceedings. Edited by D. J. Green, L. J. Gibson, and K. Sieradski. Materials Research Society, Pittsburgh, PA, 1991.

[39]R. E. Johnson, Jr., and W. H. Morrison, Jr., "Ceramic Powder Dispersion in Nonaqueous Systems"; pp. 323–48 in Advances in Ceramics, Vol. 21, *Ceramic Powder Science*. Edited by G. L. Messing, K. S. Mazdiyashi, J. W. McCauley, and R. A. Haber. American Ceramic Society, Westerville, OH, 1987.

[40]P. D. A. Mills, J. W. Goodwin, and B. W. Grover, "Shear Field Modification, of Strongly Flocculated Suspensions—Aggregate Morphology," *Colloid Polym. Sci.*, **269,** 949–63 (1991).

[41]B. D. Mosser, J. S. Reed, and J. R. Varner, "Strength and Weibull Modulus of Sintered Compacts of Spray-Dried Granules," *Am. Ceram. Soc. Bull.*, **71,** 105–109 (1992).

[42]W. F. Seyer and R. D. Walker, "Physical Chemical Properties of cis- and trans-Decahydronaphthalene," *J. Am. Chem. Soc.*, **60,** 2125–28 (1938).

[43]J. P. Rives and B. I. Lee, "The Effect of Water on the Dispersion of Alumina in Nonaqueous Media," *Colloids Surf.*, **56,** 45–58 (1991).

[44]C. A. Malbrel and P. Somasundaran, "Effect of Water on the Dispersion of Colloidal Alumina in Cyclohexane Solutions of Aerosol OT," *Langmuir*, **8,** 1285–90 (1992).